SUPPLEMENTAL MATERIALS

SUPPLEMENTAL METHODS

Ex vivo erythroid differentiation and treatments

$CD34^+$ cells were isolated from UCB within 24h of vaginal delivery of full-term infants after informed consent and approval by the "Committee for the Protection of Persons" (IRB) of the University Hospital of Montpellier. BM aspirates were obtained from deidentified donors at the Clinic Hematology Department of the University Hospital of Montpellier (CHU, Montpellier, France), as well as hip surgeries from the Tissue Donation Program at Northwell Heath and Moffitt Cancer Center & Research Institute (Tampa, FL, USA), after informed consent and approval from the respective IRBs. Healthy frozen BM was also obtained from StemCell Technologies. MDS and non-MDS patients' samples promoted at the CHU of Montpellier were obtained from the HemoDiag prospective cohort of patients with hemopathy (NCT02134574). DBA samples were obtained through the Clinical Protocol on the "Pathophysiological Explorations of Red Blood Cells" (NCT03541525, for peripheral blood) and the "Treatment of Refractory Diamond-Blackfan Anemia With Eltrombopag" (NCT04269889, for bone marrow). Marrow was collected under protocol 20-H-0021, approved under the general NIH IRB, with consents collected in accordance with the Declaration of Helsinki, the International Conference on Harmonization/GCP, and relevant parts of the Code of Federal Regulations, most notably but not limited to title 21 CFR, part 50, and title 45 CFR, part

46. $CD34^+$ cells were selected using the anti-hCD34 Microbead Kit (Miltenyi Biotech) following the manufacturer's instructions. For MDS samples, the anti-hCD34 Microbead UltraPure human kit (Miltenyi Biotech) was used. For selection of $CD34^+CD38^-$ cells, positively-selected cells were stained with an anti-CD38 mAb and FACS-sorted on a FACSAria.

Selected $CD34^+$ cells (1×10^5 cells/ml), unless otherwise indicated, were expanded in StemSpan H3000 media (StemCell Technologies Inc) supplemented with StemSpam CC100—which contains recombinant Flt3L, SCF, IL-3, and IL-6 (StemCell Technologies Inc), at 37°C with a humidified 5% CO_2 atmosphere. Cells were plated in 24-well or 48-well *Nunclon Delta surface plates (Nunc, Thermo Fisher Scientific).* After 4 days of expansion, cells were differentiated in IMDM medium (Invitrogen) supplemented with human holo-transferrin (200 mg/L, Sigma-Aldrich), human insulin (10 mg/L, Sigma-Aldrich), rhuSCF (10 ng/ml, Amgen), rhuIL-3 (1 ng/ml, R&D Systems). Erythropoiesis was induced by addition of 3 U/ml recombinant human erythropoietin (rEPO; Eprex, Janssen-Cilag), and IL-6 was removed due to its inhibitory effects on erythroid differentiation[1] (**Fig. S1A**). Cytokines were supplemented every 3-4 days, with only SCF and EPO added from day 7, as previously described.[2] Cells were centrifuged at 400g for 4 min at RT and then resuspended in fresh media to maintain cell concentrations between 0.1 and 1.5×10^6 cells/ml. For arginine deprivation experiments, IMDM for SILAC (IMDM lacking arginine and lysine, Thermo Fisher Scientific) was used supplementing the corresponding concentration of lysine (0.8 mM, Sigma-Aldrich) and arginine (0.40mM, Sigma-Aldrich) was added in the control cells.

For evaluation of the differentiation of single cell $CD34^+CD38^-$ progenitors, two assays were performed. For assessment of colony forming units (CFU), $CD34^+$ BM progenitors were cultured in SFEM with 5% FBS, containing SCF (25ng/ml), IL-3 (10ng/ml) and IL-6 (10ng/ml) for 24h. Lentiviral transduction was performed at 24h (see below) and GFP^+ $CD34^+CD38^-$ progenitors were sorted at 72h and cells were then used in the StemMACS™ HSC-CFU Assay Kit (Milteyni) as per the manufacturer's instructions. At day 14, colony images were evaluated using the EVOS M7000 and CFU were evaluated using the Milteyni standardized flow cytometry-based read-out. For evaluation of single cell colonies generated in liquid culture erythroid conditions, cells were transduced at day 1-2 and single GFP^+ $CD34^+CD38^-$ progenitors were FACS-sorted into wells of a 96 well plate 48h later in the presence of EPO (3U/ml), SCF (10ng/ml) and IL-3 (10ng/ml). Additional wells were generated with 100 and 5,000 GFP^+ $CD34^+CD38^-$ progenitors/well. Phenotypes of cells were evaluated at day 10 and day 7, respectively.

In some experiments, progenitors were differentiated in the presence of 1 mM difluoromethylornithine (DFMO, provided by Dr. Thomas Dever), 5 µM N1-Guanyl-1,7-diaminoheptane (GC7, SantaCruz Biotechnology), 10 µM N1,N11-Diethylnorespermine (DENS, Tocris), 100 µM Trans-4-Methylcyclohexylamine (MCHA, Sigma-Aldrich), 100 µM N-(3-Aminopropyl)cyclohexylamine (APCHA, SantaCruz Biotechnology), 2.5 µM AMXT-1501 tetrahydrochloride (MedChemExpress), 5 µM ciclopirox (CPX, Sigma-Aldrich), 3 mM 2-Imino-1-imidazolidineacetic acid (cyclocreatine, Sigma-Aldrich), 50 µM N^G,N^G-Dimethylarginine dihydrochloride (ADMA, Sigma-Aldrich), 5 mM chloramphenicol (CPL, Sigma-Aldrich), 5 mM diethylsuccinate (Suc, Sigma-Aldrich). 100 µM of the polyamines putrescine or spermidine (Put or Spd, Sigma-Aldrich) were added in cells treated with DMFO alone or with DFMO and AMXT-1501. Drugs were freshly added after every media change. As chloramphenicol was dissolved in ethanol

and ciclopirox in DMSO, control conditions included cultures using the same concentration of ethanol or DMSO (0.5% and 0.025%, respectively). Since cyclocreatine was dissolved in 1mM HCl, the pH of the medium was restored with 1mM NaOH.

Rps14$^{+/-}$Mx1Cre^{+} cells
Immortalized *Rps14$^{+/-}$Mx1Cre^{+}* and *Mx1Cre* murine hematopoietic progenitor cell lines were cultured in RPMI-1640, supplemented with 10%FBS, 2mM GlutaMAX, Penicillin-Streptomycin, rmuSCF (50 ng/ml) and β-estradiol (0.5 mM).

T cell activation
T cells in bone marrow aspirates were isolated from the flow-through of positively-selected CD34^{+} cells. Cells were selected using the CD3 Rosette separation kit (StemCell Technologies) following the addition of RBC (500µl). CD3^{+} T cells were then stimulated with CD3/CD28 Dynabeads (1bead/cell; Life Technologies) + rhuIL-2 (40U) in AIM-V media (Invitrogen) supplemented with 5% FBS, Penicillin-Streptomycin, HEPES and GlutaMAX for 96 hours. Unstimulated cells were maintained in rhuIL7 (1ng/ml).

Lentiviral production and transduction
Cells were transduced with the shRNA plasmids described in the Methods where the 714bp sequence encoding for EGFP was inserted in place of the puromycin gene at the unique BamHI and KpnI restriction sites. Virions were generated by transient transfection of 293T cells (2-3x106 cells/100 mm plate in 7 ml DMEM) with these vectors (10 µg) together with the Gag-Pol packaging construct PsPax2 (5 µg) and a plasmid encoding the VSV-G envelope, pCMV-VSV-G (2.5 µg), as described previously (Loisel-Meyer et al., 2012). Cells were transfected for at least 18 hours, and transfection efficiency was verified by monitoring GFP fluorescence by microscopy. Viral supernatant was harvested 24 hours post-transfection and virions were concentrated by overnight centrifugation at 4°C at 1,500g (with no break). Virions were resuspended in approximately 20 µl of RPMI with 10% FBS (per plate of cells), aliquoted and stored at -80°C. Titers were determined by serial dilutions of virus preparations on Jurkat cells and are expressed as Jurkat transducing units (TU/ml).

Prior to transduction of CD34^{+}, cells were expanded for 3 days in StemSpan medium (Stem Cell Technologies Inc) supplemented with 5% fetal bovine serum (FBS), 25 ng/ml rhuSCF (Amgen), 10 ng/ml rhuIL-3 and rhuIL-6 (R&D). 5×10^5 cells were then exposed to viral supernatants containing 4.8×10^6 TU to 9.9×10^6 TU (multiplicity of infection of 10-20). After 72h of transduction, CD34^{+} cells were cultured in presence or absence of rEPO (3 U/ml). Transduction efficiency was monitored as a function of GFP expression. For gene transfer into CD34^{+}CD38^{-} progenitors, transductions were performed at day 1-2 as described above.

Flow cytometry
Expression of surface markers was monitored on 1x10^5 cells using the indicated antibodies described in Table S1, in a total volume of 100 µl as previously described.[3,4] Cells were incubated in the dark for 20 minutes in PBS containing 2% FBS at 4ºC and then washed at 400g for 4 min. Surface GLUT1 and SLC7A1 expressions were monitored by binding to their retroviral envelope ligand (RBD) fused to eGFP for GLUT1 (1:25 dilution in 50 µl; Metafora biosystems) or to the RBD-rFc fusion protein for SLC7A1 (1:25 dilution in 50 µl) for 30 minutes in PBS containing 2% FBS at 37ºC.[5-9] RBD-rFc fusion protein incubation was followed by staining with an Alexa Fluor 488 or Alexa

Fluor 647-coupled anti-rabbit IgG antibody (1:500 dilution in 100 µl, Thermo Fisher Scientific) for 20 minutes in PBS-2% FBS at 4ºC. Phosphorylation of the ribosomal protein S6 (at S235/S236) was assessed on cells ($2x10^5$) fixed in 4% PFA (100 µL) for 30 min at RT. Cells were then resuspended in 90% cold methanol (500 µL) and kept at -20ºC until analysis. Phosphorylation was monitored using an anti-phoshoS6$^{Ser235/236}$ Ab (1:100 dilution in100 µl; Cell Signaling Technologies) for 30 minutes and revealed with a secondary rabbit IgG AlexaFluor 647-conjugated antibody (1:500 dilution in 100 µL; ThermoFisher Scientific) for 20 min at 4ºC. A minimum of 10,000 events were recorded for each acquisition on a FACS-Canto II (BD Biosciences), and data were analyzed using FlowJo software (BD Biosciences).

Quantitative Real Time PCR

Total RNA was isolated at the indicated time points and cDNA was synthetized using the RNeasy Mini Kit and the QuantiTect™ Reverse Transcription Kit (Qiagen) as per the manufacturer's instructions. Quantitative PCR of cDNAs was performed using the Quantitect SYBR green PCR Master mix (Roche) with 10 ng of cDNA (by NanoDrop) and 0.5 µM primers in a final volume of 10 µl. Primer sequences are as follows: *SLC7A1*: 5'- CTATGGCGAGTTTGGTGC -3' (forward) / 5'- CTATCAGCTCGTCGAAGGT -3' (reverse); *DHPS*: 5'- GGGTTGGCCTTTGTATCTGA-3' (forward) / 5'- TTTACAGGCCCAGATGAAGC-3' (reverse); *RPL11:* 5'- GGGAACTTCGCATCCGCAA -3' (forward) / 5'- CGCACCTTTAGACCCTTCTCC -3' (reverse); and β-actin: 5'-GTCTTCCCCTCCATCGTG-3' (forward) / 5'- TTCTCCATGTCGTCCCAG-3' (reverse). Amplification of cDNAs was performed using the LightCycler 480 (Roche). Cycling conditions included a denaturation step for 5 min at 95°C, followed by 40 cycles of denaturation (95°C for 10 sec), annealing (63°C for 10 sec) and extension (72°C for 10 sec). After amplification, melting curve analysis was performed with denaturation at 95°C for 5 sec and continuous fluorescence measurement from 65°C to 97°C at 0.1°C/s. Each sample was amplified in triplicate. Data were analyzed by LightCycler® 480 Software (Version 1.5) and Microsoft Excel. Relative expression was calculated by normalization to β-actin as indicated (delta-Ct). Real-time PCR CT values were analyzed using the 2(Delta-Delta Ct) method to calculate fold expression (ddCt).

Protein extractions and immunoblots

Protein content was extracted in RIPA lysis buffer (2.5 mM Tris-HCl pH 7.4, 1.3 mM NaCl, 0.01% NP-40, 0.5% sodium deoxycholate, 0.1% SDS, 1 mM EDTA) supplemented with protease inhibitors (10 mM NaF, 2 µg/ml aprotinin A) for 15 min at 4ºC (20 µl for $1x10^6$ cells). Samples were sonicated for 5 seconds at 40 kHz, and then centrifuged at 15,000g for 15 min at 4ºC. Supernatant was recovered and samples were prepared with 1:5 loading buffer (125mM Tris pH 6.8, 10% SDS, 20% Glycerol, 0.1% Bromophenol blue, 10% β-mercaptoethanol). Extracts were boiled for 5 min at 95ºC or heated for 2 minutes at 65ºC (OXPHOS complexes). Extracts corresponding to $1\text{-}5x10^5$ cells were loaded into a NuPAGE™ 4 to 12%, Bis-Tris, 1.0 mm, Mini Protein gel (Invitrogen, Thermo Fisher Scientific).

After electrophoresis, proteins were transferred to PVDF membranes (Thermo Fisher Scientific) for 2 hours at 250mA. Transfer efficiency was confirmed by Amido Black staining (Sigma-Aldrich). Membranes were incubated with 5% nonfat-dry milk in PBS-Tween 0.05% for 1 hour at RT. Blots were then incubated overnight at 4ºC with primary antibodies diluted in 3% nonfat-dry milk in PBS-Tween (1:2,000 Arginase 1; 1:2,000

Arginase 2; 1:2,500 anti-hypusine; 1:5,000 anti-eIF5A; 1:1,000 anti-OxPhos Rodent; 1:10,000 b-actin), and for 1 hour at RT with a peroxidase anti-rabbit or anti-mouse immunoglobulin (1:5,000-1:20,000). Blots were incubated in stripping buffer (1.5% Glycine, 0.1% SDS, pH 2.2) for 15 min at RT to remove previous antibodies. Antibodies were visualized using the Pierce™ ECL or the SuperSignal™ West Femto maximum sensitivity substrate (Thermo Fisher Scientific), and images were registered using the Amersham Imager 680.

Mitochondrial measurements

Mitochondrial biomass was assessed in a total volume of 100 µl by MitoTrackerGreen or MitoTrackerDeepRed staining (20 nM; Invitrogen, Molecular Probes), while mitochondrial transmembrane potential levels were monitored by staining with MitoTrackerRed CMXRos (50 nM; Invitrogen, Molecular Probes). Incubations were performed in the dark for 20 minutes in PBS-2% FBS at 37ºC. Enucleation was evaluated by staining with the SYTO16 nucleic acid stain (1 µM, Invitrogen, Molecular Probes) for 15 minutes in PBS-2% FBS at RT. Cell sorting was performed on a FACSARIA II SORP (BD Biosciences) using a 70 µm nozzle at a frequency of 87 kHertz and a pressure of 37 PSI. Analyses were performed on a FACS-Canto II cytometer (BD Biosciences). A minimum of 10,000 events were recorded each time. Data analyses were performed using FlowJo software (BD Biosciences).

Extracellular flux analyses

Oxygen consumption rates (OCR) and extracellular acidification rates (ECAR) were measured using the XFe-96 Analyzer (Seahorse Bioscience, Agilent). The calibration plate was filled with 200 µl Milli-Q water per well and kept at 37ºC overnight. At least 2 hours prior to the assay, water was replaced by 200 µl XF calibrant (Agilent)/ well. Culture plates were treated with 20 µl/well of 0.1mg/ml of Poly-D-Lysine (Sigma-Aldrich) for at least 1 hour at RT. Poly-D-Lysine solution was then removed and plates were washed twice with 200 µl Milli-Q water/well, dried, and kept at 4ºC until the assay was performed. For Mito Stress Test, cells (1×10^5 - 2×10^5) were placed in 50 µl XF medium (non-buffered DMEM containing 10 mM glucose and 2 mM GlutaMax, pH 7.3-7.4, Agilent), and incubated for 30 min at 37ºC. An additional 130 µl XF medium was added during the calibration time (20-30 min at 37ºC). Cells were monitored in basal conditions and in response to oligomycin (1 µM; Sigma-Aldrich), FCCP (1 µM; Sigma-Aldrich), rotenone (100 nM, Sigma-Aldrich) and antimycin A (1 µM; Sigma-Aldrich). A glycolysis stress test was performed in non-buffered DMEM without glucose and glutamine (Sigma-Aldrich). 2×10^5 cells/well were monitored in basal conditions and in response to D-glucose (10 mM, Sigma-Aldrich), oligomycin (1 µM, Sigma-Aldrich) and 2-deoxyglucose (2DG, 100 mM, Sigma-Aldrich). Wave software (Agilent) was employed for running the Seahorse assay and analysis.

Uptake assays

Cells (5×10^5) were washed twice in HBSS and starved for arginine or glutamine by incubation at 37°C in 30 µl arginine or glutamine-free IMDM for 30 min (Thermo Fisher Scientific and Sigma-Aldrich, respectively). Radiolabeled L-[3,4-3H]-Arginine monohydrochloride or L-[3,4-^{3}H(N)]-glutamine (Perkin Elmer) was added to a final concentration of 8 and 2 µM respectively (2 and 0.5 µCi in a total volume of 50 µl). Cells were incubated for 10 min at room temperature, washed twice in cold PBS containing 2%FBS (1,000g, 3 min), and solubilized in 500 µL of a 0.1% SDS solution. Cells were

incubated with 200 µM N-ethylmaleimide (NEM, Sigma-Aldrich) during the uptake to inhibit the SLC7A1-dependent arginine uptake. Radioactivity was measured in 4.5 ml liquid scintillation (Perkin Elmer) using an Hidex 300 SL counter. Each independent experiment was performed in triplicate.

Proteomics profiling

In-solution digestion: Pellets were lysed for 30 minutes at 4°C in 8 M Urea, 75 mM NaCl, 50 mM Tris-HCl pH 8.0, 1 mM EDTA, 2 µg/ml aprotinin (Sigma), 10 µg/ml leupeptin (Roche), and 1 mM phenylmethylsulfonyl fluoride (PMSF) (Sigma). Protein concentration of cleared lysate was estimated with a bicinchoninic acid (BCA) assay (Pierce). Protein disulfide bonds were reduced with 5 mM dithiothreitol (DTT) at room temperature for 1 hour, and free thiols were alkylated in the dark with 10 mM iodoacetamide (IAM) at room temperature for 45 min. The urea concentration in all samples was reduced to 2 M by addition of 50 mM Tris-HCl, pH 8.0. Denatured proteins were then enzymatically digested into peptides upon incubation first with endoproteinase LysC (Wako Laboratories) at 25 °C shaking for 2 h and then with sequencing-grade trypsin (Promega) at 25 °C shaking overnight, both added at a 1:50 enzyme:substrate ratio. Digestion was quenched via acidification to 1% formic acid (FA). Precipitated urea and undigested proteins were cleared via centrifugation, and samples were desalted using 50 mg tC18 1cc SepPak desalt cartridges. Cartridges were conditioned with 100% Acetonitrile (MeCN), 50% MeCN/0.1% FA, and 0.1% trifluoroacetic acid (TFA). Samples were loaded onto the cartridges and desalted with 0.1% TFA and 1% FA, and then eluted with 50% MeCN/0.1% FA. Eluted samples were frozen and dried via vacuum centrifugation.

TMT labeling of peptides: Desalted peptides were reconstituted in 30% MeCN/0.1% FA and the peptide concentration was quantified with a BCA assay. With 50 µg peptide input per channel, samples were labeled with a TMT11 isobaric mass tagging reagent (Thermo) as previously described.[10] Samples were reconstituted in 50 mM HEPES, pH 8.5, at a peptide concentration of 5 mg/ml. Dried TMT reagent was reconstituted in 100% anhydrous MeCN at a concentration of 20 µg/µl, added to each sample at a 1:1 TMT:peptide ratio, and allowed to rea for 1 h at 25 °C. Labeling was quenched upon addition of 5% hydroxylamine to a final concentration of 0.25%, incubating for 15 min at 25 °C. TMT-labeled samples were combined, frozen, and dried via vacuum centrifugation. This dried sample was reconstituted in 0.1% FA and desalted using a 50 mg tC18 1cc SepPak cartridge as described above. The eluted sample was frozen and dried via vacuum centrifugation.

Basic Reverse Phase (bRP) Fractionation: Labeled and combined peptides for proteome analysis were fractionated using offline basic reverse-phase (bRP) fractionation as previously described.[11] The sample was reconstituted in 900 µl bRP solvent A (2% vol/vol MeCN, 5 mM ammonium formate, pH 10.0) and loaded at a flow rate of 1 ml/min onto a custom Zorbax 300 Extend C18 column (4.6 x 250 mm, 3.5 µm, Agilent) on an Agilent 1100 high pressure liquid chromatography (HPLC) system. Chromatographic separation proceeded at a flow rate of 1 ml/min with a 96 min gradient, starting with an increase to 16% bRP solvent B (90% vol/vol MeCN, 5 mM ammonium formate, pH 10.0), followed by a linear 60 min gradient to 40% that ramped up to 44% and concluded at 60% bRP solvent B. Fractions were collected in a Whatman 2 ml 96-well plate (GE Healthcare) using a horizontal snaking pattern and were concatenated into 24 final fractions for proteomic analysis. Fractions were frozen and dried via vacuum centrifugation.

Liquid Chromatography and Mass Spectrometry: After reconstitution of dried fractions in 3% MeCN/0.1% FA to a concentration of 1 µg/µl, samples were analyzed via coupled Nanoflow LC-MS/MS using a Proxeon Easy-nLC 1000 (Thermo Fisher Scientific) and a Q-Exactive Plus Series Mass Spectrometer (Thermo Fisher Scientific). One µg of each fraction was separated on a capillary column (36-µm outer diameter × 75-µm inner diameter) containing an integrated emitter tip and heated to 50°C, followed by packing to a length of approximately 30 cm with ReproSil-Pur C18-AQ 1.9 µm beads (Maisch GmbH). Chromatography gradient consisted of solvent A (3% MeCN/0.1% FA) and solvent B (90% MeCN/0.1% FA), and the profile was 0:2, 1:6, 85:30, 94:60, 95:90, 100:90, 101:50, and 110:50 (minutes/percentage solvent B). The first 6 steps were performed at a flow rate of 200 nl/min and the last 2 at 500 nl/min. Ion acquisition was performed in data-dependent mode, acquiring HCD-MS/MS scans at a resolution of 35,000 on the top-12 most abundant precursor ions in each full MS scan (70,000 resolution). The automatic gain control (AGC) target was set to 3×106 ions for MS1 and 5×104 for MS2, and the maximum inject time to 120 ms for MS2. The collision energy was set to 30, peptide matching was set to "preferred," isotope exclusion was enabled, and dynamic exclusion time was set to 20 seconds.

Data Analysis: Mass spectrometry data was processed using Spectrum Mill (Rev BI.07.04.210, proteomics.broadinstitute.org). Extraction of raw files retained spectra within a precursor mass range of 750-6000 Da and a minimum MS1 signal-to-noise ratio of 25. MS1 spectra within a retention time range of +/- 60 s, or within a precursor m/z tolerance of +/- 1.4 m/z were merged. MS/MS searching was performed against a human UniProt database. Digestion parameters were set to "trypsin allow P" with an allowance of 4 missed cleavages. The MS/MS search included fixed modifications, carbamidomethylation on cysteine and TMT on the N-terminus and internal lysine, and variable modifications, acetylation of the protein N-terminus, oxidation of methionine, and TMT-hypusination of lysine. Restrictions for matching included a minimum matched peak intensity of 30% and a precursor and product mass tolerance of +/- 20 ppm. Peptide matches were validated using a maximum false discovery rate (FDR) threshold of 1.2%, limiting the precursor charge range to 2 to 6. Protein matches were additionally validated, requiring a minimum protein score of 0. Validated data was summarized into a protein-centric table and filtered for fully quantified hits represented by 2 or more unique peptides. Non-human contaminants and human keratins were removed.

Statistical approach: Each protein ID was associated with a log2-transformed expression ratio for every sample condition over the median of all sample conditions. After median normalization, a 2-sample moderated T test was performed on the data to compare treatment groups using an internal R-Shiny package based in the limma library. P-values associated with every protein were adjusted using the Benjamini-Hochberg FDR approach.[12]

Gene Set Enrichment Analysis (GSEA) was performed using the WebGestalt (WEB-based Gene SeT AnaLysis Toolkit) 2019 web tool.[13] Only the proteins significantly downregulated by GC7 were analyzed, using the $\log_2$-transformed ratios of GC7/control as input. Reactome was chosen as functional database applying the affinity propagation. Cytoscape software was employed for proteomics protein-protein interaction network analysis,[14] applying the STRING plugin,[15] and MCODE[16] for the clustering analysis. Analyses of mitochondrial proteins were performed using MitoMiner v4.0 (MRC, Mitochondrial Biology Unit).[17]

Statistical analysis

Data are represented as individual values or means. Error bars represent the standard error of the mean (SEM). Data were analyzed with Prism (GraphPad software). All groups followed normal distribution, and *p*-values were determined by one-way ANOVA (Tukey's post-hoc test) or t-tests, as indicated in the corresponding text and figure legends. Two-tailed t-tests were used in all figures. Tests were paired or unpaired as indicated. For proteomic analysis, data were median normalized and subjected to a 1-sample moderated t test using an internal R-Shiny package based in the limma R library. Benjamini-Hochberg FDR methods was used to correct for multiple testing. All statistical details of experiments can be found in the figure legends.

References

1. McCranor BJ, Kim MJ, Cruz NM, et al. Interleukin-6 directly impairs the erythroid development of human TF-1 erythroleukemic cells. *Blood Cells Mol Dis*. 2014;52(2-3):126-133.
2. Yan H, Hale J, Jaffray J, et al. Developmental differences between neonatal and adult human erythropoiesis. *Am J Hematol*. 2018;93(4):494-503.
3. Hu J, Liu J, Xue F, et al. Isolation and functional characterization of human erythroblasts at distinct stages: implications for understanding of normal and disordered erythropoiesis in vivo. *Blood*. 2013;121(16):3246-3253.
4. Schulz VP, Yan H, Lezon-Geyda K, et al. A Unique Epigenomic Landscape Defines Human Erythropoiesis. *Cell Rep*. 2019;28(11):2996-3009 e2997.
5. Manel N, Kim FJ, Kinet S, Taylor N, Sitbon M, Battini JL. The Ubiquitous Glucose Transporter GLUT-1 Is a Receptor for HTLV. *Cell*. 2003;115(4):449-459.
6. Kim FJ, Manel N, Garrido EN, Valle C, Sitbon M, Battini JL. HTLV-1 and -2 envelope SU subdomains and critical determinants in receptor binding. *Retrovirology*. 2004;1(1):41.
7. Swainson L, Kinet S, Manel N, Battini JL, Sitbon M, Taylor N. Glucose transporter 1 expression identifies a population of cycling CD4+ CD8+ human thymocytes with high CXCR4-induced chemotaxis. *Proc Natl Acad Sci U S A*. 2005;102(36):12867-12872.
8. Kinet S, Swainson L, Lavanya M, et al. Isolated receptor binding domains of HTLV-1 and HTLV-2 envelopes bind Glut-1 on activated CD4+ and CD8+ T cells. *Retrovirology*. 2007;4:31.
9. Ivanova S, Giovannini D, Bellis J, et al. Use of receptor-binding domain derived from bovine leukemia virus for the diagnosis or treatment of cationic l-amino acid transporter-related diseases. In: Organization WIP ed; 2017.
10. Zecha J, Satpathy S, Kanashova T, et al. TMT Labeling for the Masses: A Robust and Cost-efficient, In-solution Labeling Approach. *Mol Cell Proteomics*. 2019;18(7):1468-1478.
11. Mertins P, Tang LC, Krug K, et al. Reproducible workflow for multiplexed deep-scale proteome and phosphoproteome analysis of tumor tissues by liquid chromatography-mass spectrometry. *Nat Protoc*. 2018;13(7):1632-1661.
12. Benjamini Y, Hochberg Y. Controlling the false discovery rate: a practical and powerful approach to multiple testing. *Journal of the Royal Statistical Society*. 1995;Series B (Methodological):289-300.
13. Liao Y, Wang J, Jaehnig EJ, Shi Z, Zhang B. WebGestalt 2019: gene set analysis toolkit with revamped UIs and APIs. *Nucleic Acids Res*. 2019;47(W1):W199-W205.
14. Shannon P, Markiel A, Ozier O, et al. Cytoscape: a software environment for integrated models of biomolecular interaction networks. *Genome Res*. 2003;13(11):2498-2504.
15. Szklarczyk D, Franceschini A, Wyder S, et al. STRING v10: protein-protein interaction networks, integrated over the tree of life. *Nucleic Acids Res*. 2015;43(Database issue):D447-452.
16. Bader GD, Hogue CW. An automated method for finding molecular complexes in large protein interaction networks. *BMC Bioinformatics*. 2003;4:2.
17. Smith AC, Robinson AJ. MitoMiner v4.0: an updated database of mitochondrial localization evidence, phenotypes and diseases. *Nucleic Acids Res*. 2019;47(D1):D1225-D1228.
18. Nishiki Y, Farb TB, Friedrich J, Bokvist K, Mirmira RG, Maier B. Characterization of a novel polyclonal anti-hypusine antibody. *Springerplus*. 2013;2:421.
19. Rio S, Gastou M, Karboul N, et al. Regulation of globin-heme balance in Diamond-Blackfan anemia by HSP70/GATA1. *Blood*. 2019;133(12):1358-1370.

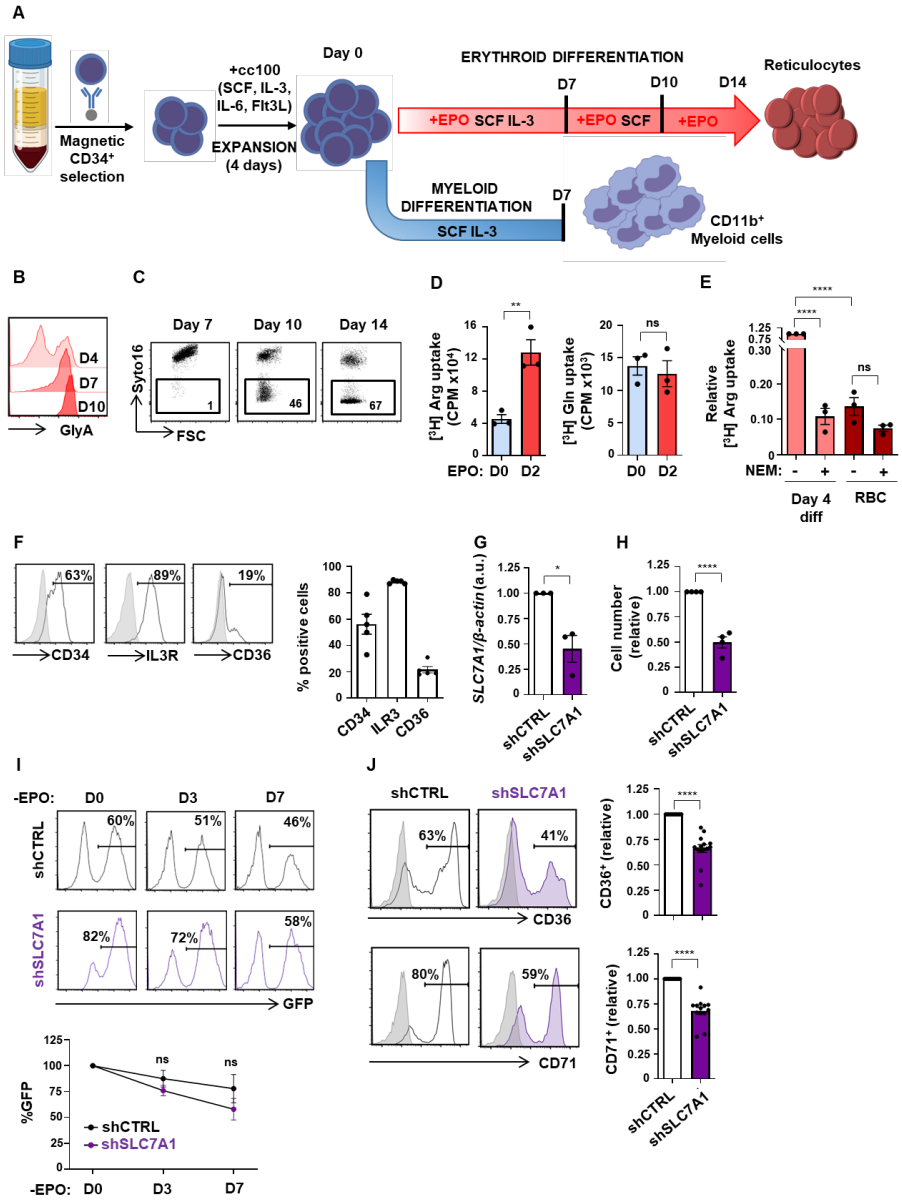

Fig. S1. Selective disadvantage of SLC7A1/CAT1-downregulated progenitors upon erythroid but not myeloid differentiation.

(**A**) Schematic representation of the *ex vivo* differentiation protocol of CD34$^+$ progenitors. Following a 4 day expansion, erythroid differentiation was induced by addition of rEPO to SCF/IL-3 while myeloid differentiation was induced in the absence of EPO (SCF/IL-3 alone). (**B**) Expression of GlyA was evaluated at days 4, 7 and 10 of differentiation and representative histograms are shown. (**C**) Enucleation was monitored at days 7, 10, and 14 as a loss of Syto16 nuclear staining and representative dot plots are presented. (**D**) Arginine and glutamine uptakes were monitored at days 0 and 2 of EPO-induced differentiation using [^{3}H] L-arginine (2 µCi) or L-[3,4-^{3}H (N)]glutamine (0.5 µCi), respectively, for 10 min at RT. Uptake is expressed as mean counts per minute (CPM) of triplicate samples ±SEM. (**E**) [^{3}H] l-arginine uptake was monitored at day 4 of differentiation as well as in mature RBC, in the absence or presence of the N-ethylmaleimide (NEM) SLC7A1 inhibitor. Mean CPM of triplicate samples in 3 independent experiments ± SEM are presented. (**F**) The phenotype of CD34$^+$ progenitors transduced at day 3 following cytokine stimulation (SCF, IL-3, and IL-6) was evaluated as a function of CD34, IL3Rα, and CD36 expression and representative histograms are shown (left). Quantifications of percent positive cells from 5 individual donors are presented. (**G**) Expression of *SLC7A1* was evaluated by qRT-PCR in shCTRL and shSLC7A1-transduced progenitors, sorted on the basis of GFP expression, and normalized to actin. Means ± SEM of 3 independent experiments are shown with values in control cells set at "1". (**H**) Relative cells numbers were evaluated at day 3 of differentiation following transduction with an shCTRL or shSLC7A1 vector (n=4). (**I**) The evolution of shCTRL- and shSLC7A1-transduced progenitors was evaluated at days 0, 3, and 7 in the absence of EPO stimulation, as a function of GFP expression, and representative histograms are presented (top). Quantification of the loss of GFP expression is presented relative to day 0, set at "100%" (n=4, bottom). (**J**) CD36 and CD71 levels were evaluated in shCTRL- and shSLC7A1-transduced progenitors at day 3 of EPO stimulation. Representative histograms are shown and quantification of positive cells were compared relative to shCTRL cells (n=14 for CD36 and n=13 for CD71). *p<0.05; **p<0.01; ****p<0.0001; ns, not significant

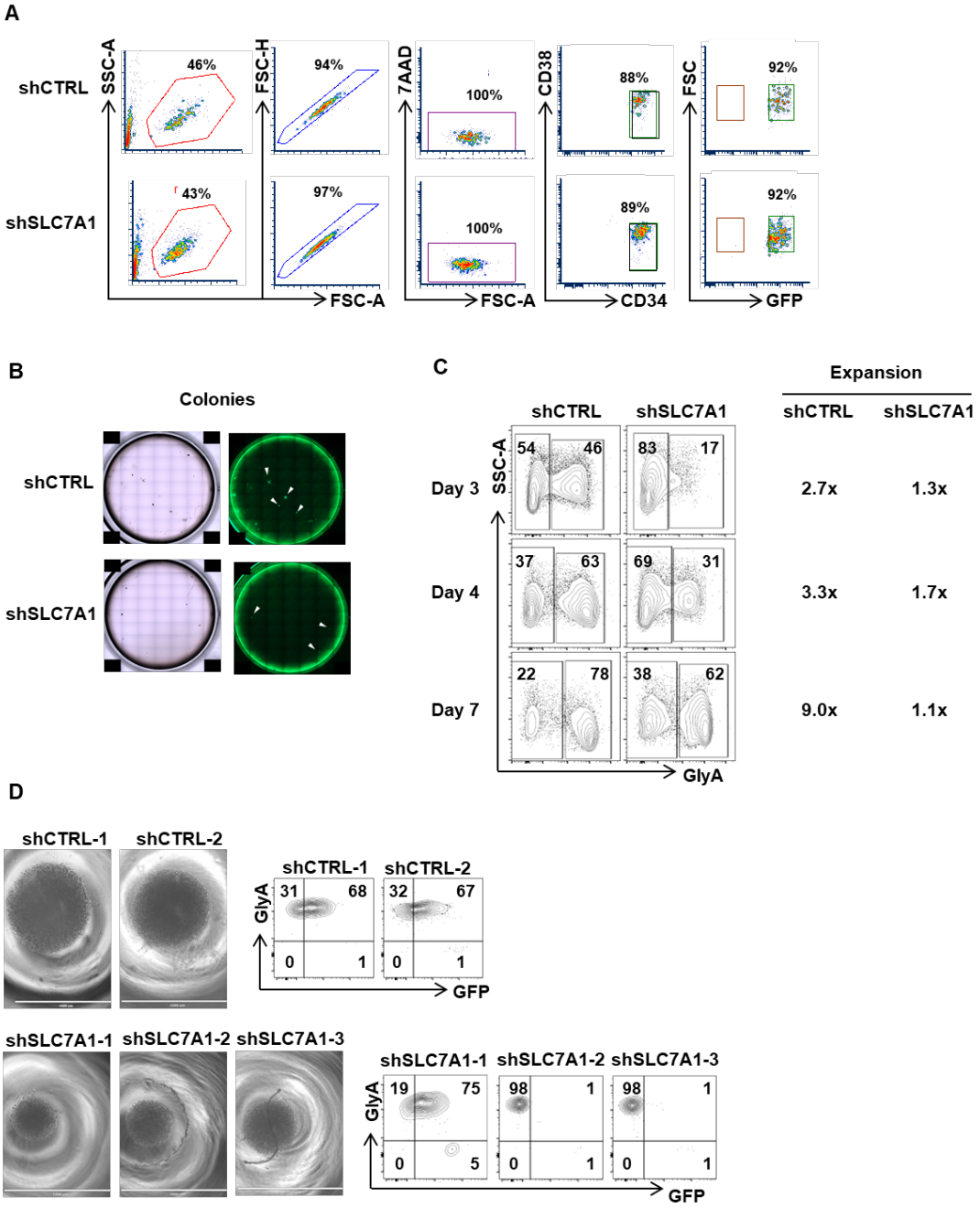

Fig. S2. CD34$^+$CD38$^-$ progenitors exhibit significantly attenuated erythroid differentiation following downregulation of SLC7A1/CAT1.

(**A**) Purified CD34$^+$ BM progenitors were transduced with shCTRL- and shCAT1-lentiviral vectors at day 1 following cytokine stimulation and transduced progenitors exhibiting a CD34$^+$CD38$^-$ phenotype were FACS-sorted at day 3 on the basis of GFP expression. Representative FACS profiles are presented (n=1 of 6 independent experiments). (**B**) CD34$^+$CD38$^-$ progenitors transduced with shCTRL and shCAT1 vectors were evaluated for CFU potential using the StemMACS™ HSC-CFU Assay Kit (Miltenyi) and representative colony images were evaluated using the EVOS M7000 imaging system. Total (left) and GFP$^+$ colonies are shown from 1 of 3 representative experiments performed in triplicate (magnification 40x). Representative GFP$^+$ colonies are indicated with arrowheads. (**C**) Purified CD34$^+$ BM progenitors were transduced with shCTRL- and shCAT1-lentiviral vectors as above and 5x10^3 transduced (GFP$^+$) CD34$^+$CD38$^-$ progenitors were seeded in 96 well plates in the presence of rEPO, SCF, and IL-3. Erythroid differentiation was monitored as a function of GlyA expression and FACS profiles are shown for days 3, 4, and 7 (left panels). Expansion of shCTRL- and shCAT1-transduced progenitors was assessed by counting of viable cells and data from 1 representative experiment are shown (right). (**D**) shCTRL- and shCAT1-transduced CD34$^+$CD38$^-$ progenitors were FACS-sorted as above, seeding 100 cells/ well. Wells were photographed at day 10 following rEPO stimulation (left) and the GFP/GlyA profiles of cells from each well were evaluated by flow cytometry (right).

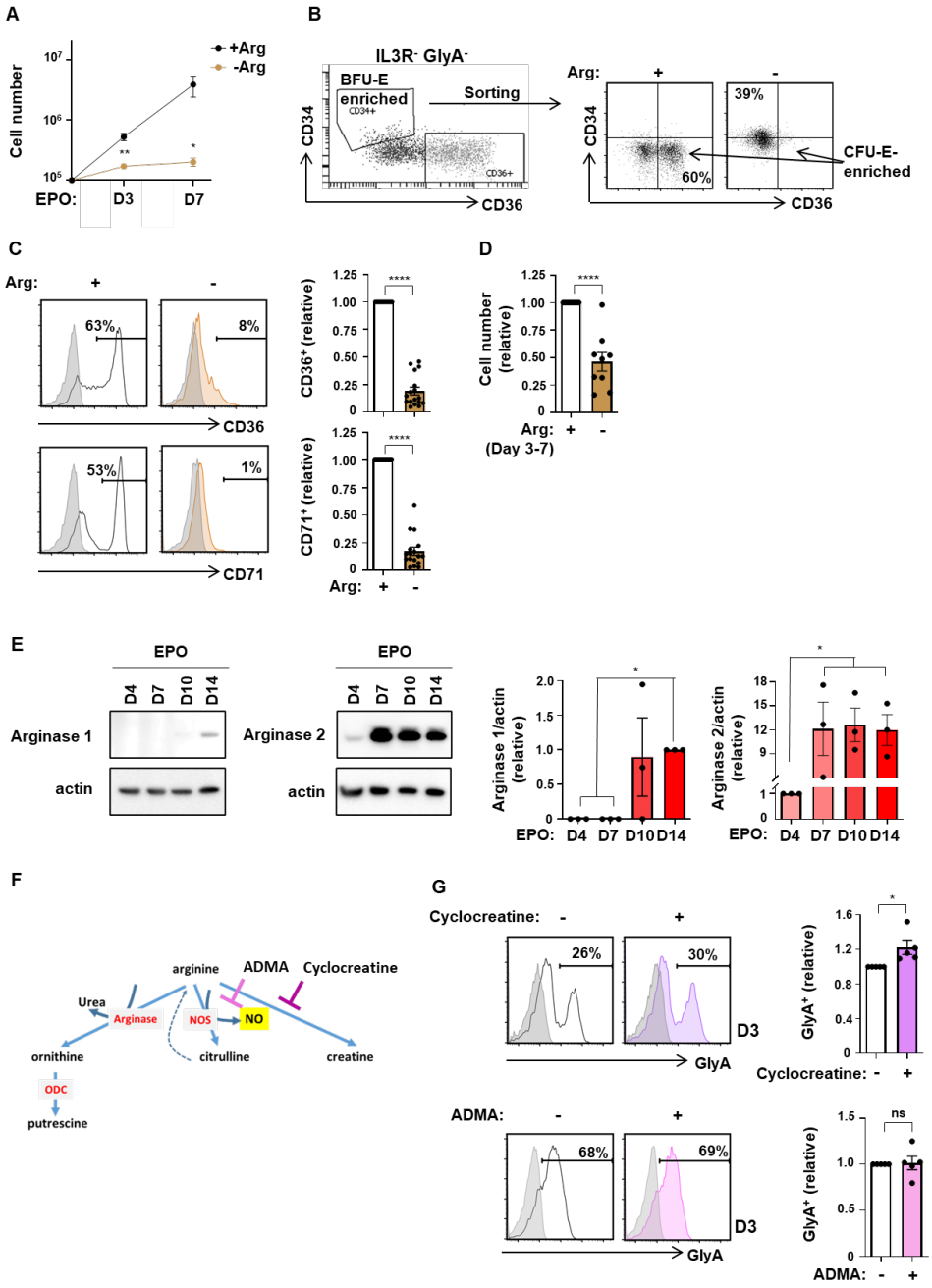

Fig. S3. Erythroid lineage specification is not dependent on arginine catabolism to NO or creatine.
(**A**) Proliferation of progenitors differentiated in EPO in the presence or absence of Arg is presented as mean cell numbers ± SEM at the indicated time points (n=8). (**B**) Representative dot plot showing CD34/CD36 profiles of IL3R$^-$ GlyA$^-$ progenitors, distinguishing between BFU-E-enriched (CD34$^+$CD36$^+$) and CFU-E-enriched (CD34$^-$CD36$^+$) cells are shown. Sorted BFU-E were differentiated in the presence or absence of arginine (Arg) and CD34/CD36 profiles were evaluated 4 days later (right). (**C**) CD36 and CD71 expression were evaluated at day 3 of EPO-induced differentiation in the presence or absence of Arg. Representative histograms (left) and quantification of relative levels (right, n=17) are presented. (**D**) Progenitors were differentiated for 3 days in the presence of EPO and differentiation was then continued in the presence or absence of Arg until day 7. Cell numbers relative to the presence of Arg are presented (n=9). (**E**) Expression of arginase 1 and 2 were evaluated at days 4, 7, 10, and 14 of erythroid differentiation and representative immunoblots as well as actin immunoblots are shown (left). Quantification of arginase expression relative to actin was evaluated, and levels of Arg1 at day 14 were arbitrarily set at "1", and Arg2 levels at day 4 were arbitrarily set at "1" (n=3). (**F**) Schematic showing the generation of putrescine, citrulline, NO, and creatine from arginine. Enzymes are shown in red and cyclocreatine, an analog of the creatine and inhibitor of the creatine biosynthesis as well as asymmetric dimethylarginine (ADMA), a competitive inhibitor of nitric oxide synthase (NOS), were used to inhibit these respective pathways. (**G**) The impact of cylocreatine (top, 3mM) and ADMA (bottom, 50µM) on erythroid differentiation was evaluated as a function of GlyA staining at day 3 and representative histograms (left) as well as quantification of GlyA expression (n=5) are presented (right).*p<0.05; **p<0.01 ****p<0.0001; ns, not significant

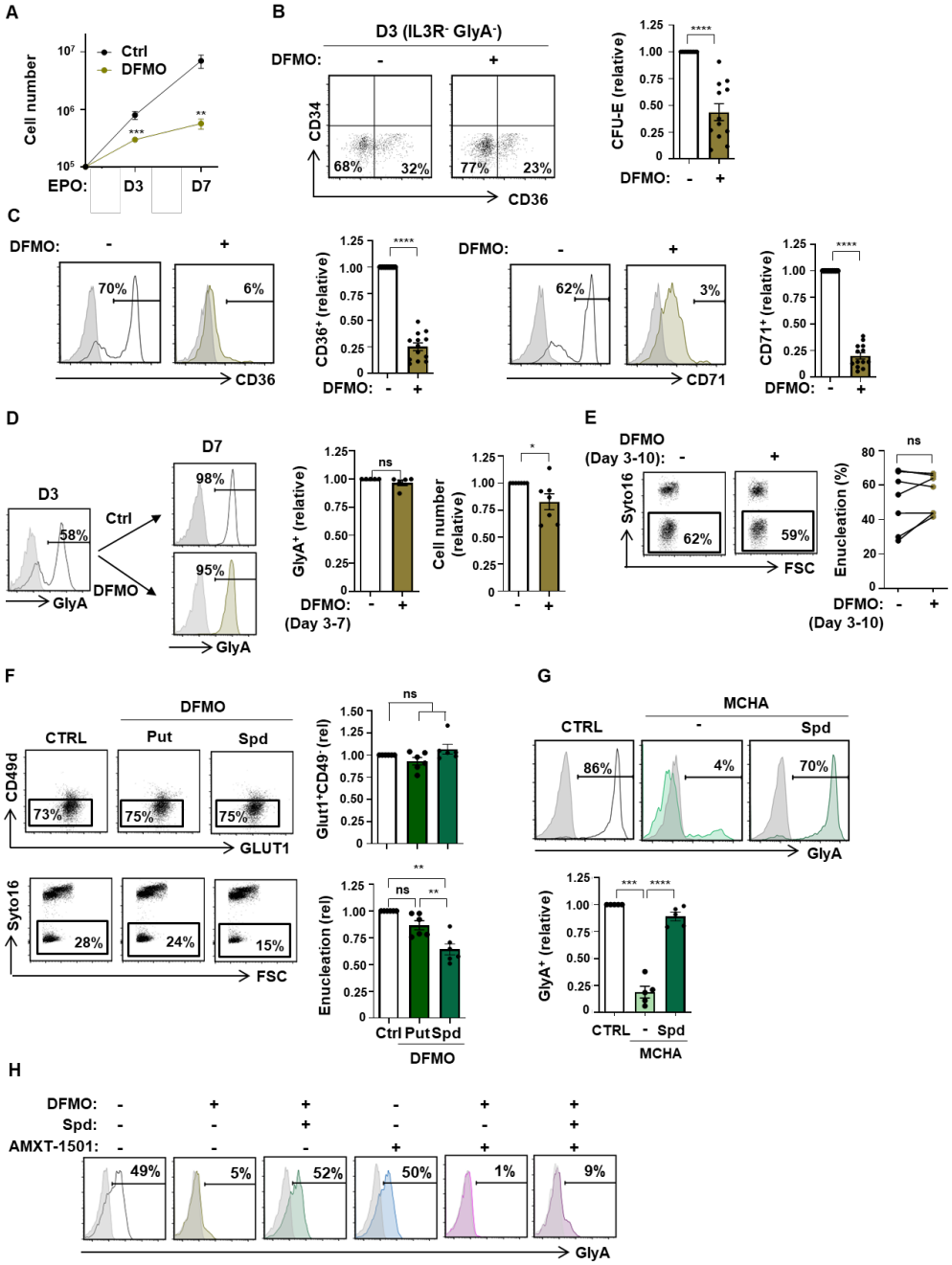

Figure S4. Spermidine rescues erythroid differentiation in the absence of polyamine biosynthesis.
(**A**) Proliferation of progenitors differentiated in EPO in the absence or presence of 1mM DFMO is presented as mean cell numbers ± SEM at the indicated time points (n=13). (**B**) Representative dot plots of CD34/CD36 profiles of IL3R$^-$ GlyA$^-$ cells are shown for progenitors differentiated in the absence or presence of DFMO (day 3) and the percentages of IL3R$^-$GlyA$^-$CD34$^-$CD36$^+$ (CFU-E) are indicated (left). Quantification of CFU-E relative to the absence of DFMO are presented (n=12, right). (**C**) Differentiation was monitored as a function of CD36 and CD71 expression in the presence or absence of DFMO and representative histograms are presented (left). Quantification of expression relative to control conditions are shown (right, n=13). (**D**) Progenitors were differentiated in the presence of EPO until day 3 and then differentiation was continued in the absence or presence of DFMO. Representative histograms showing GlyA expression at days 3 and 7 are presented (left). Quantification of GlyA expression (middle, n=5) and cell counts (right, n=7) are presented. (**E**) Following EPO-induced differentiation between days 3 and 10, in the absence or presence of DFMO, enucleation was monitored as a function of Syto16 staining. Representative dot plots (left) and comparisons of enucleation levels in 7 independent experiments (right) are shown. (**F**) The impact of DFMO and polyamines on late erythroblast differentiation (top) and enucleation (bottom) was evaluated at day 10 of differentiation. Representative CD49d/GLUT1 (top left) and Syto16 (bottom left) profiles as well as quantifications (right) (n=6) are shown. (**G**) MCHA-treated progenitors were differentiated with rEPO in the presence of absence of spermidine. Representative histograms (top) and quantifications (n=5, bottom) are presented. (**H**) Erythroid differentiation was induced in the presence or absence of DFMO, spermidine (100µM) and AMXT-1501 (2.5µM) and representative histograms showing GlyA expression at day 3 are presented. *p<0.05; **p<0.01; ***p<0.001; ****p<0.0001; ns, not significant

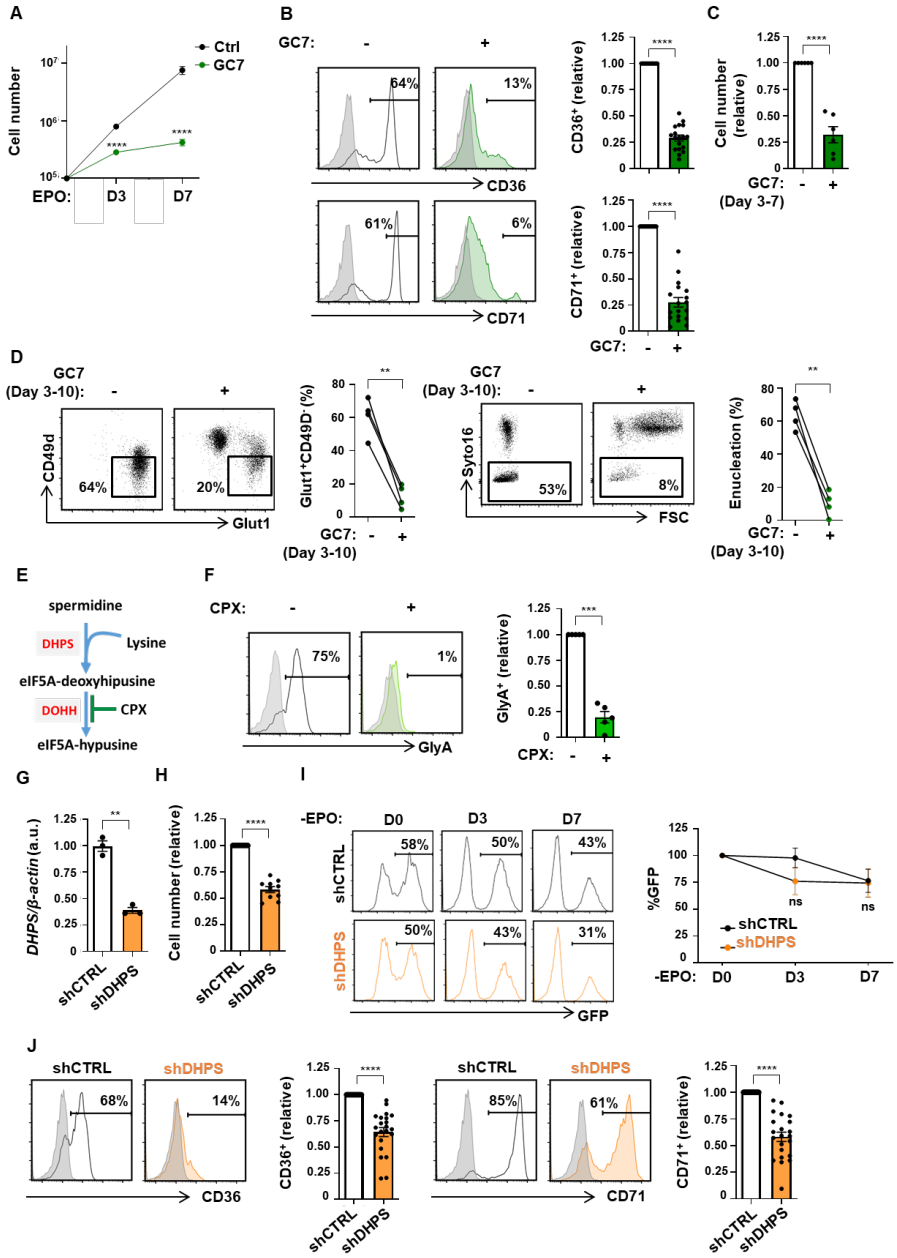

Fig. S5. Myeloid differentiation is not inhibited by DHPS downregulation.
(**A**) Proliferation of progenitors differentiated in EPO in the absence or presence of GC7 (5µM) is presented as mean cell numbers ± SEM at the indicated time points (n=17). (**B**) Erythroid differentiation was monitored as a function of CD36 and CD71 expression and representative histograms are shown (left). Quantification of expression relative to control conditions is presented (n=18, right). **(C)** Progenitors were differentiated for 3 days and then exposed to GC7 for days 3-7. Cell numbers at day 7, relative to control conditions are shown (n=6). (**D**) Differentiation of GlyA$^+$ cells was monitored as a function of a CD49d$^-$Glut1$^+$ phenotype at day 10 and representative dot plots (left) as well as percentages in the absence or presence of GC7 are shown (left, n=4). Enucleation was monitored as a function of Syto16 staining (right, n=4). (**E**) Schematic showing the generation of eIF5a^H from spermidine, as a function of the catalytic activities of DHPS and DOHH. Inhibition of DOHH by ciclopirox (CPX) is presented. (**F**) Erythroid differentiation in the absence or presence of CPX (5µM) was evaluated at day 3 of differentiation as a function of GlyA expression and representative histograms are shown (left). GlyA expression relative to control conditions is presented (n=5, right). (**G**) Expression of DHPS was evaluated by qRT-PCR in shCTRL- and shDHPS-transduced progenitors as a function of actin and means ± SEM of 3 independent experiments are shown. (**H**) Cell numbers were monitored at day 3 of differentiation and are presented relative to shCTRL-transduced progenitors (n=10). (**I**) Evolution of shCTRL- and shDHPS-transduced progenitors was monitored as a function of co-expressed GFP under conditions of non-erythroid (myeloid) differentiation. Representative histograms at the indicated time points are shown (left). Quantification of GFP expression relative to day 0 is shown (right, n=3). (**J**) CD36 (left) and CD71 (right) expression was monitored in shCTRL- and shDHPS-transduced progenitors at day 3 of differentiation and representative histograms are shown. Expression relative to controls conditions was evaluated and means ± SEM are presented (n=22). **p<0.01; ***p<0.001; ****p<0.0001; ns, not significant

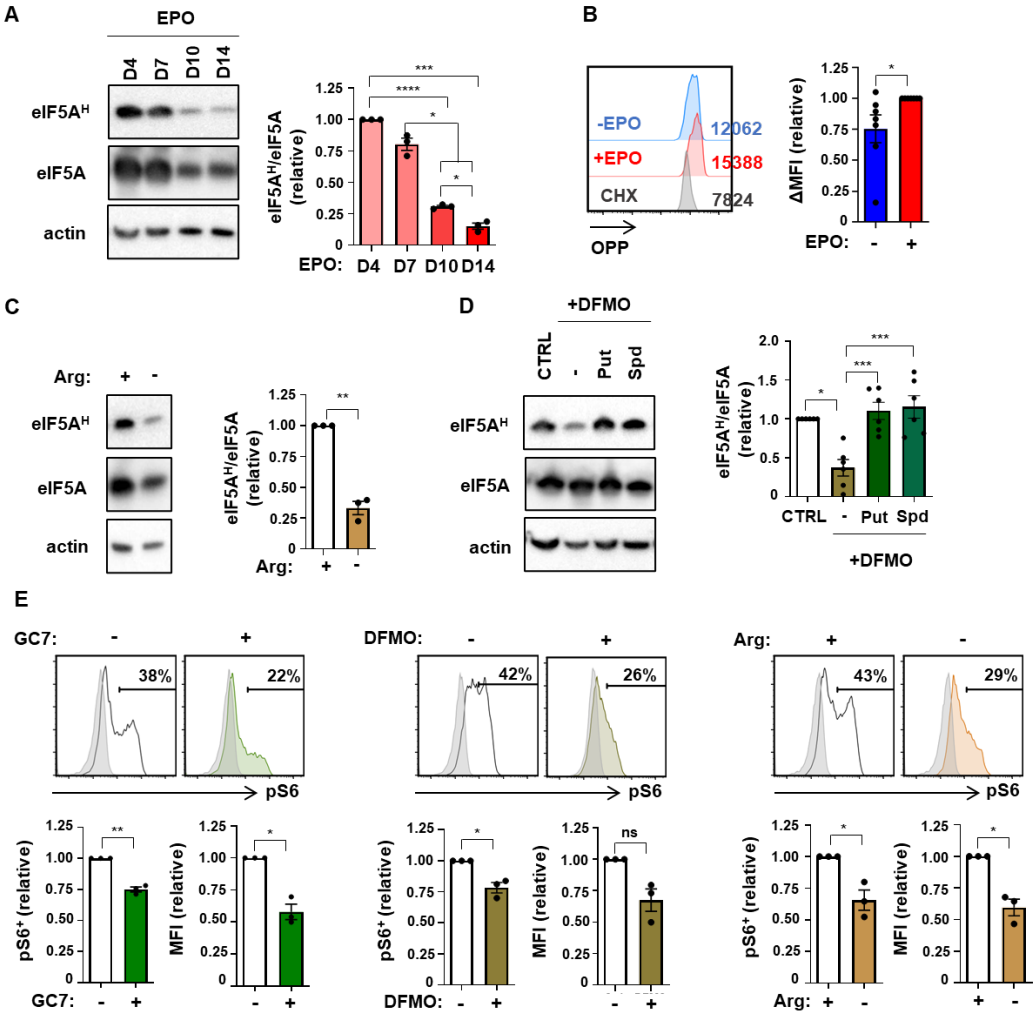

Fig. S6. Arginine metabolism regulates hypusination of eIF5A in erythroid progenitors.
(**A**) Hypusination of eIF5A was evaluated at days 4, 7, 10 and 14 of erythroid differentiation by immunoblotting with a polyclonal antibody against hypusinated human eIF5A (eIF5A^{H}). Control immunoblots assessing total eIF5A protein and actin are presented (left). Quantification of hypusine relative to eIF5A was determined, with levels at day 4 arbitrarily set at 1 (n=3, right). (**B**) Protein synthesis was monitored by OPP and representative histograms in the presence or absence of EPO as well as in the presence of cycloheximide (CHX, 1µM) are presented (left) and MFIs are indicated (right). Quantification of changes in OPP relative to EPO conditions are shown (n=7). (**C**) Hypusine levels were evaluated following differentiation in the presence or absence of arginine and immunoblots (left) as well as quantification (n=3, right) are shown. (**D**) Hypusination was evaluated at day 3 of erythroid differentiation in control conditions as well as in the presence of 1mM DFMO, either alone or supplemented with 100µM putrescine (Put) or spermidine (Spd). Representative immunoblots (left) and quantifications of eIF5A^{H} /eIF5A are shown (right, n=6). (**E**) Phosphorylation of the S6 ribosomal protein, an mTOR downstream effector, was monitored 24h following treatment of EPO-induced progenitors in the presence of GC7, DFMO, or in arginine-deprived conditions. Representative histograms (top) are presented with isotype staining presented in grey. The percentages of p-S6^{+} cells ± SEM are presented (bottom, n=3). *p<0.05; **p<0.01; ***p<0.001; ****p<0.0001; ns, not significative

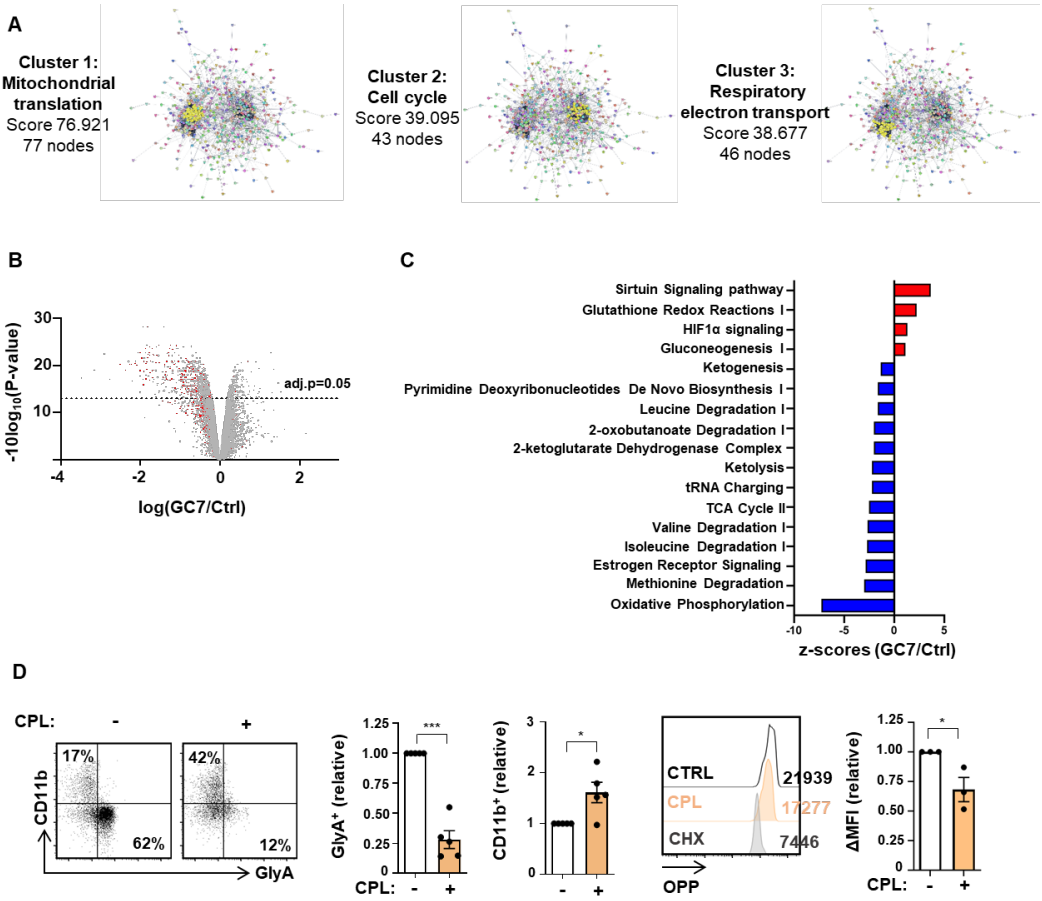

Fig. S7. Inhibition of eIF5A hypusination results in a significant inhibition in the synthesis of mitochondrial proteins.

(**A**) PPI network clustering analysis identified mitochondrial translation, cell cycle and respiration electron transport pathways as significantly downregulated in the presence of 5μM GC7. Scores and nodes are indicated. (**B**) A volcano plot showing differences in GC7-mediated protein expression (Log2FC), with all mitochondrial proteins presented in red. Of 824 mitochondrial proteins, 620 were downregulated and 204 were upregulated. (**C**) Pathway analysis of mitochondrial proteins identified in the proteomics screen. Pathways upregulated and downregulated by GC7 are presented in red and blue, respectively. (**D**) Erythroid differentiation was monitored at day 3 in the absence or presence of chloramphenicol (CPL, 5mM) as a function of CD11b/GlyA expression and representative dot plots and quantification (n=5) are presented (left). Protein expression in these conditions was monitored by OPP staining at day 1 of differentiation and representative histograms and quantification (n=3) are shown (right). *p<0.05; ***p<0.001.

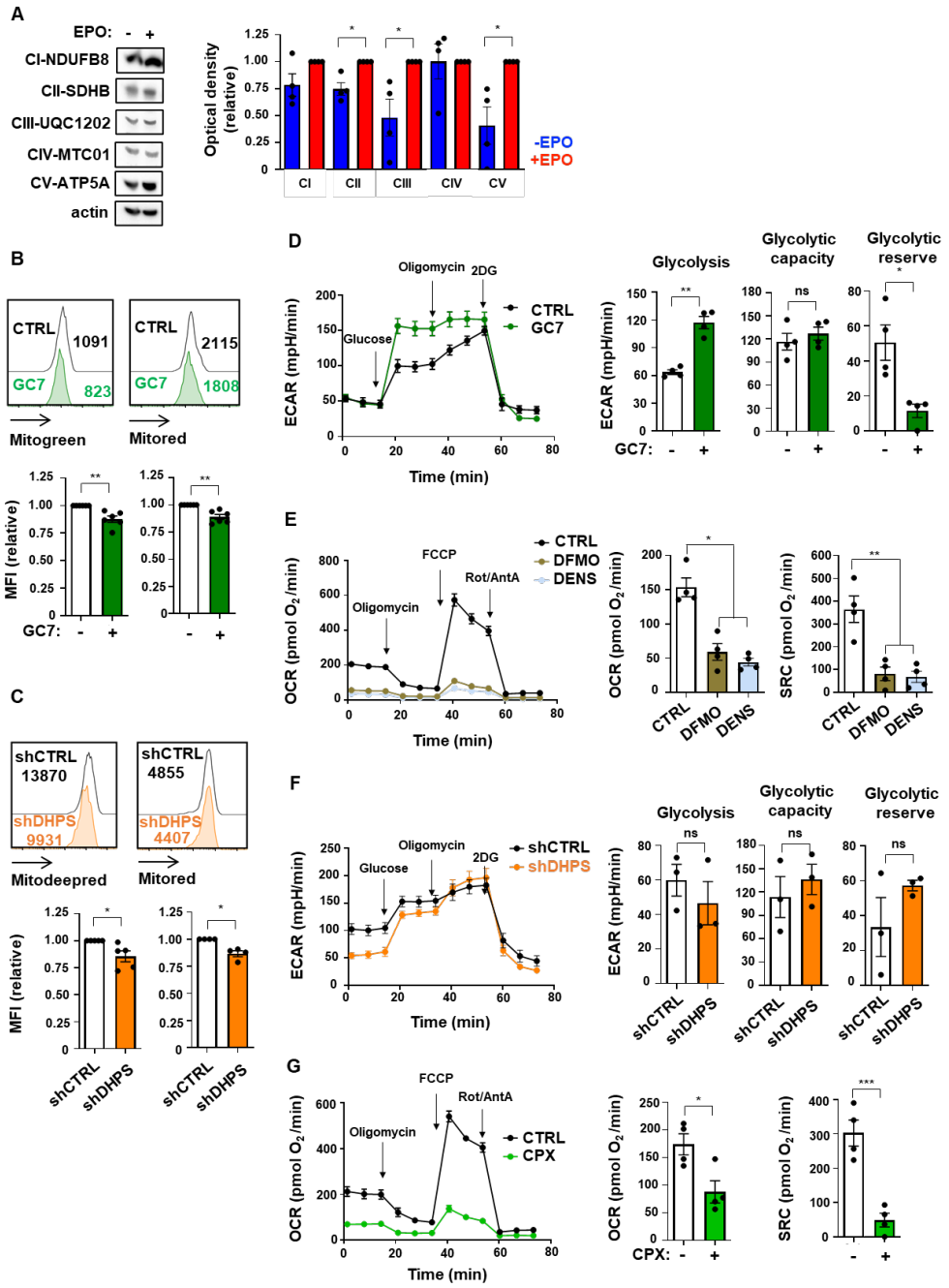

Fig. S8. Hypusinated eIF5A regulates oxidative phosphorylation in hematopoietic progenitors.
(**A**) Mitochondrial complexes (CI to CV) were monitored on progenitors differentiated for 4 days in the presence or absence of EPO. Representative immunoblots (left) and quantifications (relative to EPO-treated progenitors) are presented (n=4, right). (**B**) Mitochondrial biomass and polarization were monitored as a function of Mitotracker green and Mitotracker red staining, respectively, and representative histograms (top) and quantifications (bottom, n=6) are shown for progenitors differentiated in the absence or presence of GC7 (day 1). (**C**) shCTRL- and shDHPHS-transduced progenitors were stained with Mitotracker deepred and Mitrotracker red at day 1 of differentiation and representative histograms (top) as well as quantification of staining relative to shCTRL cells (bottom, n=4-5) are shown. (**D**) A glycolysis stress test was performed to evaluate the impact of 5µM GC7 treatment on glycolysis and a representative tracing at day 1 of differentiation is shown (left). Glycolysis, glycolytic capacity, and glycolytic reserve were evaluated using the Agilent Seahorse XF assay and means ± SEM are presented (means of 4 independent experiments performed with 3-6 technical replicates) (right). (**E**) OCR was monitored on day 1 of erythroid differentiation in the absence or presence of 1mM DFMO or 10µM DENS and a representative tracing (left) as well as means ± SEM of basal OCR and SRC in 4 independent experiments (with 3-6 technical replicates each) are presented (right). (**F**) A glycolysis stress test was performed on shCTRL- and shDHPS-transduced progenitors at day 1 of differentiation as in panel D and glycolysis, glycolytic capacity and glycolytic reserve are presented (n=3). A representative tracing (left) and means ± SEM are presented (right). (**G**) OCR was monitored on day 1 of erythroid differentiation in the absence or presence of 5µM CPX and means ± SEM of basal OCR and SRC in 4 independent experiments (with 3-6 technical replicates each) are presented (right). *p<0.05; **p<0.01; ***p<0.001; ns, not significant

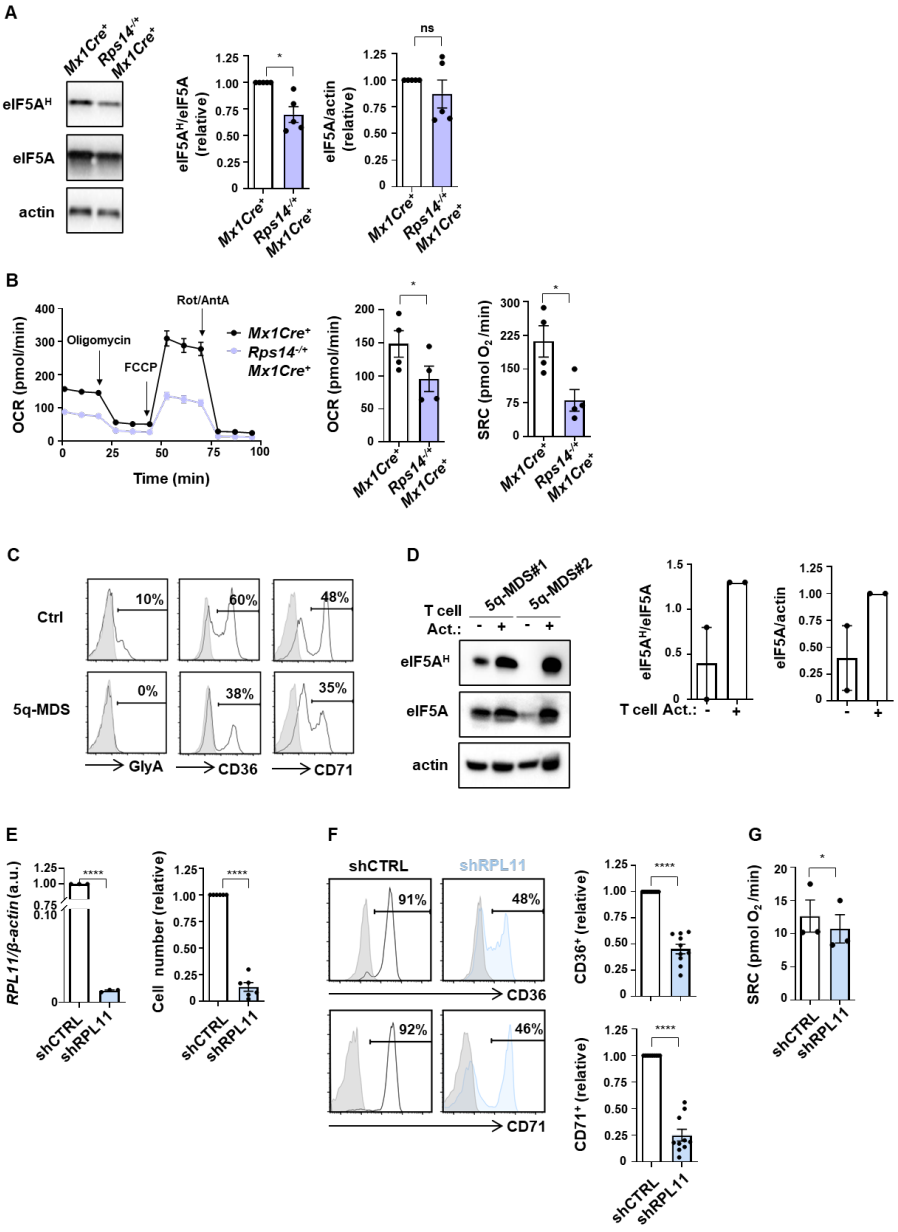

Figure S9. The defective erythroid differentiation associated with ribosomal protein insufficiency is linked to impaired hypusination.

(**A**) Hypusination and total eIF5A levels were evaluated in immortalized erythroid bone marrow progenitors generated from control Mx1Cre^{+} and RPS14 haploinsufficient Rps14$^{+/-}$Mx1Cre^{+} mice (Schneider et al., 2016). Representative immunoblots (left) and quantifications of eIF5A^{H}/eIF5A and eIF5A/actin levels are presented (right, n=5). (**B**) OCRs of immortalized Mx1Cre^{+} and Rps14$^{+/-}$Mx1Cre^{+}progenitors were evaluated and representative data (left, n=6 technical replicates) (n=4 independent experiments, right panel) are presented. SRC levels ± SEM (n=4) are presented for data presented in panel 7B in *Mx1Cre*$^{+}$ and *Rps14*$^{+/-}$*Mx1Cre*$^{+}$ progenitors. (**C**) Expression of GlyA, CD36, and CD71 were evaluated in BM progenitors from a healthy control individual and a del(5q)-MDS patient at day 3 of erythroid differentiation. (**D**) Induction of eIF5A hypusination in T lymphocytes from two del5q-MDS patients was assessed 96h following CD3/CD28 stimulation, relative to unactivated lymphocytes. Immunoblots showing hypusinated and total eIF5A as well as actin are presented (left) and quantifications of the eIF5A^{H}/eIF5A and eIF5A/actin ratios are presented (right). (**E**) Expression levels of RPL11 were evaluated by qRT-PCR following transduction with shRPL11 virus (left). mRNA levels were normalized to actin and means ± SEM in 3 independent experiments are shown with values in control cells set at "1." Total cell numbers were evaluated at day 3 of differentiation and are presented relative to shCTRL conditions (right, n=6). (**F**) CD36 (top) and CD71 (bottom) were evaluated in shCTRL- and shRPL11-transduced progenitors at day 3 of EPO stimulation. Representative histograms are shown (left) and quantification of positive cells were compared relative to shCTRL cells (right, n=10). (**G**) SRC levels ± SEM are presented for shCTRL- and shRPL11-transduced progenitors (n=3 independent experiments). *p<0.05; ****p<0.0001; ns, not significant

Table S1. Patient Characteristics

Patient	Sex	Age	Mutations	Diagnosis	Treatment
5q-MDS #1	Male	65	Del(5q) Somatic mutation in *SREB1*	Refractory anemia with excess blasts (6% blasts)	Lenalidomide
5q-MDS #2	Female	75	Del(5q) Somatic mutations in *TP53*, *MPL* and *MAP3K14*	Refractory anemia with excess blasts (3.8% blasts)	-
5q-MDS #3	Female	68	Del(5q) Somatic mutation in *ASXL1*	Refractory anemia with excess blasts (16.5% blasts)	-
Ctrl #1	Female	82	2 mutations in *TET2* (22% and 36%)	Neutropenia, microcytic anemia No MDS	-
Ctrl #2	Male	73	*U2AF1* 4%, *CEBPA* 2.9%, *TET2* 29.3% *CBL* 17%	Refractory anemia with excess blasts (10% blasts)	-
Ctrl #3	Female	67	-	Anemia and thrombopenia	-

Patient	Sex	Age	Mutation	Bone marrow cellularity	Retic count, $\times 10^9$/L	Platelet count x10^9/μL	Hg g/dL	ARC$\times 10^9$/μL	Malformations	Characteristics for treatment	Treatment
DBA#1	Female	16	*RPL11* c.27_28 delGA(p.N10FS) Pathogenic as all but the first 10aa are disrupted	Hypocellular marrow of 50% with a M:E ratio of 3-4:1	-	260	10.9	45.7	-	Steroid-refractory	Transfusion q3weeks
DBA#2	Female	37	*RPL11 (NM_000975):* c.164dup ; p.(Tyr55Ter) Class 4 variant-Likely pathogenic by ACMG criteria; Pathogenic criteria weighted as very strong (PVS1) and supporting (PM2)	-	48.4	Normal range	7.6	-	-	Steroid-intolerant	Transfusion q2months
Ctrl#1	Female	20									
Ctrl#2	Male	30									

Table S2. Reagent list

REAGENT/RESOURCE	COMPANY/SOURC	REFERENCE
Antibodies		
Anti-hCD11b-PE (clone Bear1)	Beckman Coulter	Cat#IM2581U ; *RRID* : AB_131334
Anti-hCD34-FITC (clone 581)	Becton Dickinson	Cat#55582 ; RRID :AB_396150
Anti-hCD34-APC (clone 581)	Becton Dickinson	Cat#555824 ; *RRID* :AB_398614
Anti-hCD34-PE (clone 581)	Beckman Coulter	Cat#A07776
Anti-hCD36-APC (clone FA6.152)	Beckman Coulter	Cat#A87786
Anti-hCD36-FITC (clone FA6.152)	Beckman Coulter	Cat#B49201 ; *RRID* :AB_2848117
Anti-hCD36-PB (clone FA6.152)	Beckman Coulter	Cat#B43302
Anti-hCD38-FITC (clone T16)	Beckman Coulter	Cat#A07778 *RRID* :AB_2909810
Anti-hCD38-PC7 (clone HIT2)	eBioscience/ThermoFisher	Cat# 25-0389 *RRID* :AB_1724065
Anti-hCD49d-APC (clone HP2/1)	Beckman Coulter	Cat#B01682
Anti-hCD71-APC (clone MA-A712)	Becton Dickinson	Cat#551374 ; *RRID* :AB_398500
Anti-hCD71-APC-AF750 (clone MA-A712)	Beckman Coulter	Cat#A89313 ; *RRID* :AB_2800452
Anti-hGlyA-PC7 (clone 11^{E}4B-7-6)	Beckman Coulter	Cat#A71564 ; *RRID* :AB_2800449
Anti-hGlyA-APC (clone GA-R2 (HIR2))	eBioscience/ThermoFisher	Cat#17-9987 42 ; *RRID* :AB_2043823
Anti-hIL3R-PC7 (clone 6H6)	eBioscience/ThermoFisher	Cat#25-1239-42 ; *RRID* :AB_1257136
Anti-Arginase 1 (D4E3M™)	Cell Signaling Technology	Cat#93668S *RRID* : AB_2800207
Anti-Arginase 2 (D9J1N)	Cell Signaling Technology	Cat#55003S *RRID* : AB_2799475
Anti-Hypusine polyclonal antibodies	Reference[18]	
Anti-eIF5A (Clone 26/eIF-5a)	Becton Dickinson	Cat#611976 *RRID* : AB_399397
OXPHOS Rodent WB Antibody Cocktail	Invitrogen/Thermo Fisher	Cat#45-8099 *RRID* : AB_2533835
Anti-beta-actin (Clone AC74)	Sigma-Aldrich	Cat#A5316 *RRID* : AB_476743
Anti-phospho-S6 Ribosomal Protein (Ser235/236) (D57.2.2E)	Cell Signaling Technology	Cat#4858S RRID : AB_916156
Goat anti-Rabbit IgG Alexa Fluor 488	Molecular Probes/ThermoFisher	Cat#A-11008 *RRID* : AB_143165
Goat anti-Rabbit IgG Alexa Fluor 647	Molecular Probes/ThermoFisher	Cat#A-21244 *RRID* : AB_2535812
Goat anti-Rabbit IgG, HRP-linked	Cell Signaling Technology	Cat#7074S *RRID :* AB_2099233

Goat anti-Mouse IgG HRP-linked	Cell Signaling Technology	Cat#7076S *RRID :* AB_330924
GLUT1 RBD-GFP	Metafora Biosystems	Cat#GLUT1_G100
CAT1 RBD-rFc	Metafora Biosystems	
Bacterial and Virus Strains		
Top 10 Competent Cells	ThermoFisher	Cat#C404010
Biological Samples		
Human umbilical cord blood	Unité De Thérapie Cellulaire de Montpellier	N/A
Human bone marrow samples	Hématologie clinique -CHU Montpellier (HemoDiag prospective cohort) Moffitt Cancer Center & Research Institute (Tampa, FL, USA)	NCT02134574
Chemicals, Recombinant Proteins		
Difluoromethylornithine (DFMO)	Sigma-Aldrich	Cat# 288500-M
N1-Guanyl-1,7-diaminoheptane (GC7)	SantaCruz Biotechnology	Cat#SC-396111
N1,N11-Diethylnorespermine (DENS)	Tocris	Cat#6618
Trans-4-Methylcyclohexylamine (MCHA)	Sigma-Aldrich	Cat#CDS019932
N-(3-Aminopropyl)cyclohexylamine (APCHA)	SantaCruz Biotechnology	Cat#SC-202715
AMXT-1501 tetrahydrochloride	MedChemExpress	Cat#HY-124617A
Ciclopirox (CPX)	Sigma-Aldrich	Cat#SML2011
2-Imino-1-imidazolidineacetic acid (cyclocreatine)	Sigma-Aldrich	Cat#377627
N^G,N^G-Dimethylarginine dihydrochloride (ADMA)	Sigma-Aldrich	Cat#D4268
L-Arginine	Sigma-Aldrich	Cat#A5006
L-Lysine	Sigma-Aldrich	Cat#L5501
Putrescine dihydrochloride (Put)	Sigma-Aldrich	Cat#P7505
Spermidine (Spd)	Sigma-Aldrich	Cat#S2626
Chloramphenicol (CPL)	Sigma-Aldrich	Cat#C0378
Cycloheximide (CHX)	Sigma-Aldrich	Cat#C7698
Diethylsuccinate (Suc)	Sigma-Aldrich	Cat#112402
N-Ethylmaleimide(NEM)	Sigma-Aldrich	Cat#E3876
L-[3,4-3H]-Arginine monohydrochloride	Perkin Elmer	Cat#NET1123250UC
L-[3,4-3H(N)]-Glutamine	Perkin Elmer	Cat#NET551250UC
Oligomycin	Sigma-Aldrich	Cat# 75351
Carbonyl cyanide-*p*-trifluoromethoxyphenylhydrazone (FCCP)	Sigma-Aldrich	Cat#C2920
Rotenone	Sigma-Aldrich	Cat#R8875
Antimycin A (AntA)	Sigma-Aldrich	Cat#A8674
D-Glucose monohydrate	Sigma-Aldrich	Cat#49159
2-deoxy-glucose (2-DG)	Sigma-Aldrich	Cat#D6134

7-Aminoactinomycin D (7AAD)	Sigma-Aldrich	Cat#SML1633
Dimethyl sulfoxide (DMSO)	Sigma-Aldrich	Cat#D2650
Human recombinant IL-2 (Proleukin IL-2)	Clinigen Group PLC	Cat#76310-022-01
Human recombinant IL-3	R&D Systems	Cat#203-IL-010
Human recombinant IL-6	R&D Systems	Cat#206-IL-010
Human recombinant IL-7	Cytheris	Cat#CYT107
rhuSCF	Amgen	N/A
rmuSCF	PeproTech	Cat#250-03-200UG
Stem Spam CC100	Stem Cell	Cat#02690
EPREX	Janssen	Cat#3400936992368
Human holo-transferrin	Sigma-Aldrich	Cat#T0665
Human insulin solution	Sigma-Aldrich	Cat#9278
Heparin	Sanofi	Cat#3400930484500
β-estradiol	Sigma-Aldrich	Cat#E2758-250MG
Dynabeads™ Human T-Activator CD3/CD28 for T Cell Expansion and Activation	Life Technologies /Thermo Fisher	Cat#11141D
Bovine serum albumin	Sigma-Aldrich	Cat#A8806
Fetal Bovine Serum	Eurobio	Cat#CVFSVF0001
Penicillin/ Streptomycin	Life Technologies / Thermo Fisher	Cat#15140-22
IMDM	Life Technologies /ThermoFisher	Cat#21980032
IMDM for SILAC (without arginine and lysine)	Thermo Fisher	Cat#88367
IMDM wo glutamine	Sigma-Aldrich	Cat#I3390
DMEM	Sigma-Aldrich	Cat#49159
RPMI-1640 GlutaMAX™	Life Technologies /Thermo Fisher	Cat#61870036
StemSpam™ SFEM	Stem Cell	Cat#09650
StemSpam™ H3000	Stem Cell	Cat#09850
AIM-V	Life Technologies /Thermo Fisher	Cat#12055-091
Seahorse XF Assay Medium	Agilent Technologies	102365-100
Seahorse XF Calibrant Solution	Agilent Technologies	100840-000
Ultima Gold liquid scintillation cocktail	Perkin Elmer	Cat#6013329
Commercial Assays		
Anti-hCD34 MicroBead kit	Miltenyi Biotec	Cat#130-046-702; *RRID*:AB_2848167
Anti-hCD34 Microbead UltraPure kit (2x200uL)	Miltenyi Biotec	Cat#130-100-450
StemMACS™ HSC-CFU	Miltenyi Biotec	Cat#130-091-281
RosetteSep™ Human T Cell Enrichment Cocktail	StemCell Technologies	Cat# 15061
RNeasy Mini kit	Qiagen	Cat# 74104
QuantiTect™ Reverse Transcription Kit	Qiagen	Cat# 205311
Click-iT ™ Plus OPP Alexa Fluor ™ 488 Protein Synthesis Assay Kit	Molecular Probes/Thermofisher	Cat#C10456

Click-iT ™ Plus OPP Alexa Fluor ™ 647 Protein Synthesis Assay Kit	Molecular Probes/Thermofisher	Cat#C10458
Cell Lines		
Jurkat E6-1	ATCC	TIB-152
293 T cells	ATCC	CRL-3216
Immortalized *Mx1Cre*$^{+}$ progenitors	Larson laboratory (NCI, Bethesda, MD)	N/A
Immortalized *Rps14*$^{+/-}$*Mx1Cre*$^{+}$ progenitors	Larson laboratory (NCI, Bethesda, MD)	N/A
Oligonucleotides		
SLC7A1 forward: 5'-CTATGGCGAGTTTGGTGC-3'	IDT	Custom order
SLC7A1 reverse: 5'-CTATCAGCTCGTCGAAGGT -3'	IDT	Custom order
DHPS forward : 5'-GGGTTGGCCTTTGTATCTGA-3'	IDT	Custom order
DHPS reverse: 5'-TTTACAGGCCCAGATGAAGC-3'	IDT	Custom order
RPL11 forward: 5'-GGGAACTTCGCATCCGCAA-3'	IDT	Custom order
RPL11 reverse: 5'-CGCACCTTTAGACCCTTCTCC-3'	IDT	Custom order
βactin forward: 5'-GTCTTCCCCTCCATCGTG-3'	IDT	Custom order
βactin reverse: 5'-TTCTCCATGTCGTCCCAG-3'	IDT	Custom order
Recombinant DNA		
TRC1pLKO shSLC7A1	Sigma Aldrich	Cat# TRCN000042967
TRC2pLKO shDHPS	Sigma Aldrich	Cat# TRCN0000330717
TRC2pLKO shDHPS	Sigma Aldrich	Cat# TRCN0000330796
pLKO Non-Mammalian shRNA Control	Sigma Aldrich	Cat# SHC002
pRRL-eGFP-shRPL11	Reference[19]	N/A
pRRL-eGFP-Non-Mammalian shRNA Control	Reference[19]	N/A
Softwares		
FlowJo (Version 10)	BD Biosciences	https://www.flowjo.com/
Prism (Version 8)	GraphPad Software	https://www.graphpad.com/scientific-software/prism/
Wave (Version 2)	Agilent Technologies	https://www.agilent.com/en/product/cell-analysis/real-time-cell-metabolic-analysis/xf-

		software/seahorse-wave-desktop-software-740897
ImageJ	NIH	https://imagej.nih.gov
Spectrum Mill MS Proteomics Workbench (Version BI.07.04.210)	Agilent Technologies	https://www.agilent.com/en/product/software-informatics/mass-spectrometry-software/data-analysis
WEB-based GEne SeT AnaLysis Toolkit (WebGestalt) 2019	Zhang Lab (Baylor College of Medicine, Houston, TX)	https://webgestalt.org
Cytoscape (Version 3.8.2)	Institute for Systems Biology, Seattle, WA	https//cytoscape.org
Other		
MitoTracker™ Deep Red FM	Molecular Probes/Thermofisher	Cat#M22426
MitoTracker™ Green FM	Molecular Probes/Thermofisher	Cat#M7514
MitoTracker™ Red CMXRos	Molecular Probes/Thermofisher	Cat#M7512
Syto16™	Molecular Probes/Thermofisher	Cat#S7578